

3-2-2 Effects of Transequatorial Thermospheric Wind on Plasma Bubble Occurrences

SAITO Susumu and MARUYAMA Takashi

Data from the ionosonde chain in Southeast Asia (Kototabang, Indonesia (0.2°S, 100.3°E), Chumphon, Thailand (10.7°N, 99.4°E), and Chiang Mai, Thailand (18.8°N, 98.9°E)) were analyzed for a period from October, 2004 to April, 2005 to compare the bottomside ionospheric height (the virtual height at 2.5 MHz: h'F) variation and the plasma bubble occurrence. The results show that plasma bubbles were observed when the h'F enhancements around sunset at all three stations were strong. However, even when h'F enhancement near the magnetic equator (Chumphon) was strong, plasma bubbles were not observed when there was a noticeable north-south asymmetry of h'F. The north-south asymmetry in the bottomside ionospheric heights could be attributed to the strong transequatorial thermospheric neutral wind. Our results show that the strong transequatorial thermospheric wind is one of the important factors that control the day-to-day variability of the plasma bubble occurrence.

Keywords

Plasma bubble, Equatorial spread F, Day-to-day variation of plasma bubble occurrence, Transequatorial thermospheric wind, SEALION ionosonde network

1 Introduction

Plasma bubbles are low-latitude, equatorial geomagnetic phenomena that in an ionosonde observation appear as intense range-type spread F (equatorial spread F or ESF). The term “range-type spread F” refers to an obscure appearance of traces of F-region echoes across an entire frequency band, possibly caused by a scattering of ionosonde radio waves due to various scales of ionospheric irregularities.

Today, the physical mechanism of plasma bubbles is the Rayleigh-Taylor instability in plasmas. Plasma bubbles are known to form when the ionospheric is significantly uplifted by an intense ionospheric electric field moving eastward towards the sunset in what is known as “prereversal enhancement (PRE).” However, a definite correspondence between the intensity of PRE and the formation of plasma bubbles does not always exist[1], and a

plasma bubble may or may not form even where intense PRE is present. Day-to-day variations of plasma bubble occurrence are significantly marked so that the frequency of plasma bubbles forming is well-known to depend on the season, longitude, solar activity and other factors, but still leave some room for further clarification. Various physical mechanisms that dominate the relation between the intensity of PRE and the formation of plasma bubbles have been suggested to date, but none has yet to yield a definite solution.

Maruyama and Matuura [2] conducted analyses using satellite-based topside sounding (satellite-borne ionosonde) data and found that seasonal and longitudinal changes in ESF occurrence have a close bearing on the geometry of latitude distributions of plasma density, and that ESF is frequently observed when plasma density has symmetric latitude distributions with respect to the magnetic latitude. They thought that the north-south asymmetry

of plasma density is a consequence of meridional winds (transequatorial winds) among all thermospheric winds blowing past the magnetic equator, and that transequatorial winds might be increasing the plasma density of the downwind bottomside ionosphere, thereby enhancing Pedersen conductivity integrated along the magnetic lines of force to suppress the generation of ESF [3]. While the magnetic declination is longitude-specific, thermospheric zonal winds are governed more by geographic coordinates than magnetic coordinates, and the angle formed by the magnetic meridional plane and average thermospheric winds varies from longitude to longitude and season to season. This was considered one factor that could govern seasonal and longitudinal changes at ESF occurrence. Mendillo et al. [4] thought that transequatorial winds might also influence day-to-day variations in ESF occurrence, and thus conducted simultaneous 630.0 nm airglow and ALTAIR radar observations at the Kwajalein Atoll to find a relation between the north-south structure of airglow and ESF occurrence. However, thermospheric wind observations carried out by Mendillo et al. [5] using a Fabry-Perot interferometer revealed no definite relation between transequatorial winds and ESF occurrence. Valadares et al. [6] compared the north-south structure of the total electron content (TEC) with the formation of plasma bubbles by using a north-south chain of GPS receivers installed on the west coast of South America, and found that no definite relation exists between them. Analyses conducted using more data [7] yielded similar results. However, Lee et al. [8] found that a weak north-south asymmetry of TEC and an intense eastward electric field are necessary for plasma bubbles to form. Abdu et al. [9] also suggested the possibility of meridional winds working to suppress the formation of plasma bubbles, based on ionosonde observations made at two stations — one on the magnetic equator and the other in a low-magnetic-latitude region. Thus, whether transequatorial thermospheric winds play a significant role in the formation of plasma bubbles still

remains disputable.

Transequatorial thermospheric winds are not easy to observe directly, but a set of ionosondes installed on the magnetic equator and at north-south magnetic conjugate points across the equator can observe ionospheric height variations for distinguishing height variations caused by electric fields and those caused by thermospheric winds, and also be used to estimate velocity and polarity (southward, northward, equatorward convergence or poleward divergence) [3]. To this end, an ionospheric observation network called the “Southeast Asia Low-latitude Ionospheric Network (SEALION)” was set up in Southeast Asia [10] [11]. The present study explores the relation between the thermospheric meridional winds observed by SEALION and the day-to-day variations of plasma bubble occurrence.

This report is based on the work of Saito and Maruyama [12] published in *Annales Geophysicae* in 2006.

2 Observations

The present study used data collected from simultaneous observations conducted at three observation stations [at Kototabang, Indonesia (0.2°S, 100.3°E), Chumphon, Thailand (10.7°N, 99.4°E), and Chiang Mai, Thailand (18.8°N, 98.9°E)] aligned approximately along the magnetic meridional plane and across the magnetic equator among the ionosonde stations that make up the SEALION ionospheric observation network. Referring to the data summarized in Figure 1 and Table 1, Chumphon is located near the magnetic equator, whereas Kototabang and Chiang Mai are close to their respective magnetic conjugate points. The ionosondes employed were of the FM-CW (frequency modulated-continuous wave) type; these devices transmit radio waves continuously while sweeping a frequency range from 2 MHz to 30 MHz, and receive reflected waves from the ionosphere. Since the reflected waves had been emitted earlier corresponding to the time of travel to and from the ionos-

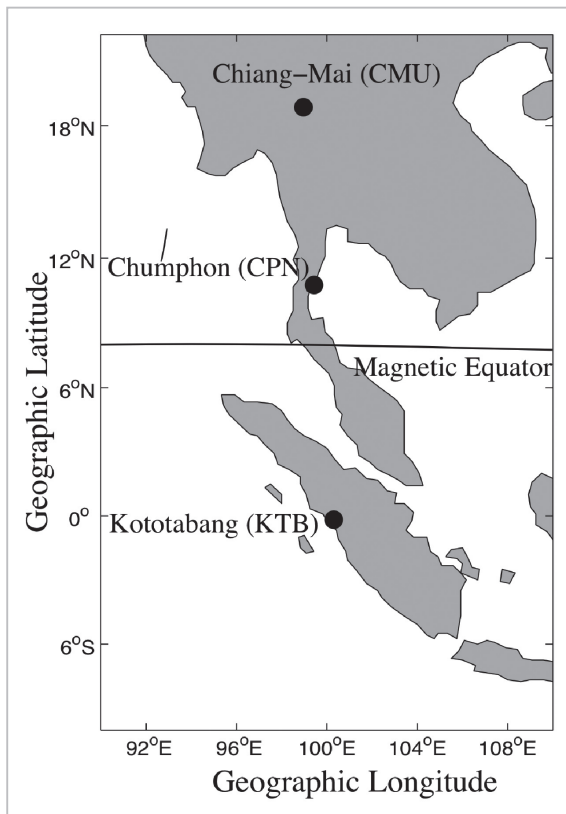


Fig. 1 Ionosonde station locations [12]

where, these waves have a somewhat lower frequency than the transmitted waves then emitted. This frequency difference can be used to measure distance to the reflecting point. A plot of the heights of reflecting points relative to frequencies is called an ionogram. Because radio waves are reflected at the point where the plasma frequency matches the radio wave frequency, electron density distributions below the peak electron density can be determined. Table 2 summarizes the ionosonde observation parameters used in the present study. Observations are iterated every five minutes to obtain an ionogram or electron density distributions in the bottomside ionosphere. The upper-limit frequency at Kototabang is limited to 20 MHz to suppress radio interference to other observation equipment.

3 Analytical method

Height variations in the ionospheric F-region are determined by the ionospheric elec-

Table 1 Locations of ionosonde stations

Observation Station	Geographic latitude	Geographic longitude	Magnetic latitude	Magnetic equatorial height of magnetic field line at altitude of 300 km
Chumphon	10.72°	99.37°	3.22°	315 km
Kototabang	- 0.20°	100.32°	-10.10°	474 km
Chiang Mai	18.76°	98.93°	13.21°	576 km

Table 2 Ionosonde observation parameters

Type	Frequency modulated-continuous wave (FM-CW) (Switched between transmission and reception by pseudo-random code)
Transmitting power (peak)	20 W
Transmitting power (average)	10 W
Frequency sweep range	2 to 30 MHz (2-20 MHz only at Kototabang)
Frequency sweep rate	100 kHz s ⁻¹
Sweep repetition period	5 min

tric field, dynamic force caused by neutral winds, and ionic chemical reaction. The work of Bittencourt and Abdu [13] revealed that variations in the ionospheric F-region virtual height ($h'F$) directly read from an ionogram provide a good indication of ionospheric movement after sunset. The ionospheric E- and F1-regions dominated by molecular ions having a high rate of extinction are rapidly extinguished after sunset, making retardation in radio propagation in these regions virtually negligible, with the virtual height of radio waves reflected at the bottom of the ionospheric F-region near the actual height. For the purpose of the present study, the authors decided to manually scale the value of $h'F$ at 2.5 MHz (corresponding to electron density of $7.75 \cdot 10^{10} \text{ m}^{-3}$) for analysis. Scaling the values of $h'F$ observed at the three stations provides insight into the latitude structure of electron density in the bottomside ionosphere. Ionograms were collected every five minutes, $h'F$ was scaled every 15 minutes, and the ionograms collected were referenced as needed. At heights up to 300 km, apparent ionospheric height variations caused by an ion chemical reaction are known to be non-negligible [13]. Actually, it is not uncommon for $h'F$ at 2.5 MHz to fall short of 300 km. Even in such a situation, apparent height variations should fully suffice for a qualitative discussion of ionospheric dynamics, unless converted to a velocity as a subject of quantitative debate.

The presence of a plasma bubble can be detected from an ionogram. If a plasma bubble exists, the radio waves from the ionosondes would be scattered by ionospheric irregularities on various associated space scales, thereby obscuring the reflection height in the ionogram over a broad frequency range in the height direction. This phenomenon is known as “range-type equatorial spread F (ESF).” A range-type ESF signifies the presence of ionospheric irregularities in the bottomside ionosphere, but not all cases of ESF indicate the formation of plasma bubbles. Probing into ESF at the three stations aligned in the magnetic meridional plane that includes the mag-

netic equator should help to clarify their latitude structure. Plasma bubbles form over the magnetic equator and grow simultaneously in the height direction and poleward along magnetic lines of force. Accordingly, the authors have decided to assume that plasma bubbles causing ESF meet the following two conditions: (1) Intense ESF is observed at all three stations. The term intense ESF refers to an ionogram in the F-region appearing obscure in the height direction to such extent that it loses its characteristic form near the critical frequency associated with peak electron density. Figure 2 illustrates an example of intense ESF. (2) ESF is first observed at Chumphon (closest to the magnetic equator) and then observed with some time lag at Kototabang and Chiang Mai. If ESF was only observed at Chumphon, ionospheric irregularities were assumed to remain in the bottomside ionosphere and not having reached the plasma bubble. Plasma bubbles are known to form around sunset in the F-region above the magnetic equator and travel eastward [14]. Hence, those observed at an early timing after sunset may have formed near an observation station, and those observed at a later time may have formed remotely from an observation station and then traveled over the observation station. For the

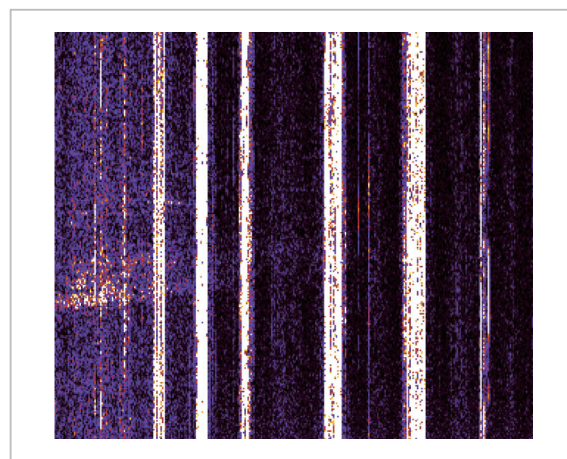


Fig.2 Example of intense spread F. The frequency is taken on the axis of abscissa, with virtual height ($h'F$) on the axis of ordinate. Marked vertical lines shown in the individual frequencies are external interference waves.

present study, the plasma bubbles observed at 19 to 21 hours LT after sunset were assumed to be “fresh” plasma bubbles forming in the vicinity of an observation station, and those observed later were assumed to be “fossil” plasma bubbles that formed remotely and then traveled along. While “fresh” plasma bubbles have presumably been formed under the influence of ionospheric conditions near the observation stations, the formation of “fossil” plasma bubbles is unlikely to be closely related to conditions near the observation stations. In other words, where only a “fossil” plasma bubble was observed at an observation station, no plasma bubble should be assumed to have formed in the vicinity of that observation station. For this reason, the authors classified the individual days into two categories—the days on which “fresh” plasma bubbles were observed, and the days on which only “fossil” plasma bubbles or no plasma bubbles were observed—for the purpose of probing the relation between the formation of plasma bubbles and ionospheric conditions.

4 Findings

The present study employed the values of $h'F$ and the formation or non-formation of ESF as read from ionograms observed at the three SEALION observation stations (Fig. 1, Table 1) in October 2004 and from March to April 2005 as data regarding plasma bubbles that frequently form in the Southeast Asian region around the vernal (spring) equinox and autumnal equinox. Figure 3 plots the maximum values of $h'F$ registered at Chumphon in association with PRE, along with the values of $h'F$ recorded at Kototabang and Chiang Mai when the value of $h'F$ was maximized at Chumphon. Where the values of $h'F$ at Kototabang and Chiang Mai were not readable under the influence of shielding by the sporadic E-layer or other conditions, data interpolated from the values of $h'F$ read from ionograms collected every five minutes was used instead. Each black circle in the diagram points to a date on which a “fresh” plasma

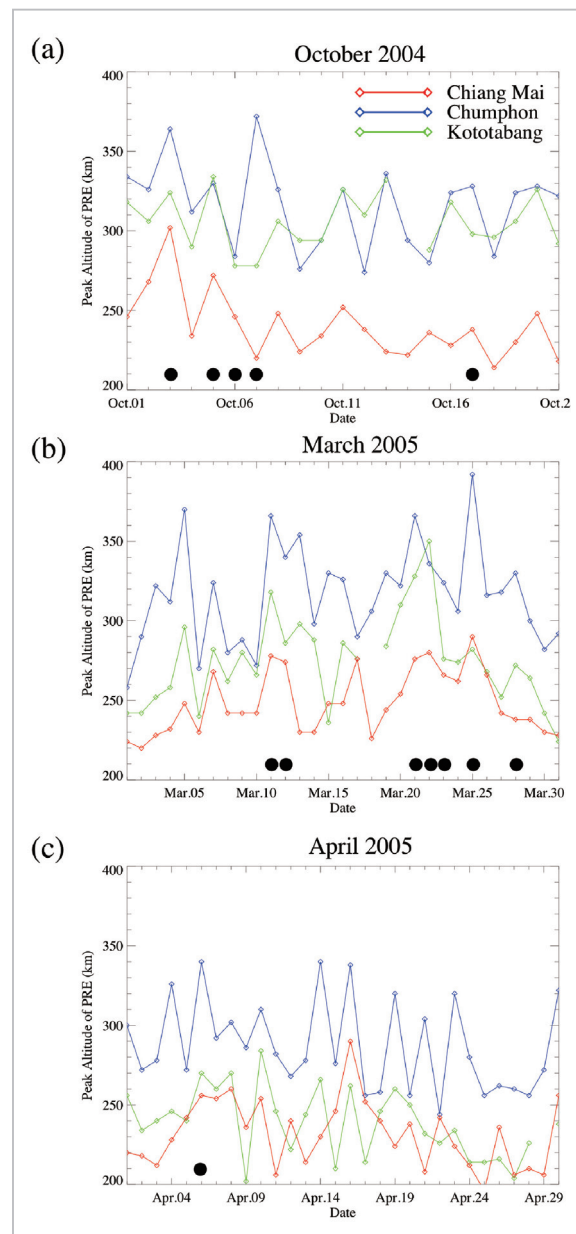


Fig.3 Values of maximum $h'F$ (blue line) on the magnetic equator (Chumphon) in (a) October 2004, (b) October 2005, and (c) April 2005) [12]. The green and red lines denote the values of $h'F$ registered at Kototabang and Chiang Mai when the value of $h'F$ was maximized at Chumphon, respectively. Each black circle signifies a “fresh” plasma bubble being observed on that date [12].

bubble was observed. The days on which a “fresh” plasma bubble was observed have an obvious tendency to exhibit a higher value of maximum $h'F$ at Chumphon than on days

when no “fresh” plasma bubbles were observed. Days on which no “fresh” plasma bubbles were observed are also noticeable, even when Chumphon registered a higher value of maximum h’F. What is the difference between the two instances of observation and non-observation of “fresh” plasma bubbles when Chumphon posted a higher value of maximum h’F? The difference is found in the values of h’F registered at Kototabang and Chiang Mai (remote from the magnetic equator). The ionosphere is found to have been lifted over Kototabang and Chiang Mai, as well as Chumphon closer to the magnetic equator, on days when only “fresh” plasma bubbles were observed.

This may be more evidently understood by looking at time-related variations in h’F at the three observation stations (Fig. 4). Figure 4 breaks down individual days into three categories: (a) days when “fresh” plasma bubbles were observed, (b) days when “fresh” plasma bubbles did not form and the maximum value of h’F at Chumphon exceeded 325 km, and (c) days when “fresh” plasma bubbles did not form and the maximum value of h’F at Chumphon fell short of 325 km. It also plots variations in average h’F at each of the three observation stations. Increases in h’F (ionosphere lift) associated with PRE were noticed at all three observation stations on days when “fresh” plasma bubbles formed [Fig. 4 (a)]. On days when h’F rose significantly at Chumphon but no “fresh” plasma bubbles were observed [Fig. 4 (b)], Chiang Mai registered a significantly small increase in h’F, as compared to a rise at Kototabang to equal Chumphon on days when “fresh” plasma bubbles were observed. This means that electron density in the bottomside ionosphere had a north-south asymmetrical structure with respect to the magnetic equator. Fig. 4 (c) plots the values of h’F recorded when PRE was weak. “Fresh” plasma bubbles were not observed even once in such a situation. Figure 5 shows that the differences in h’F between Kototabang and Chiang Mai are obviously pronounced around the PRE maxi-

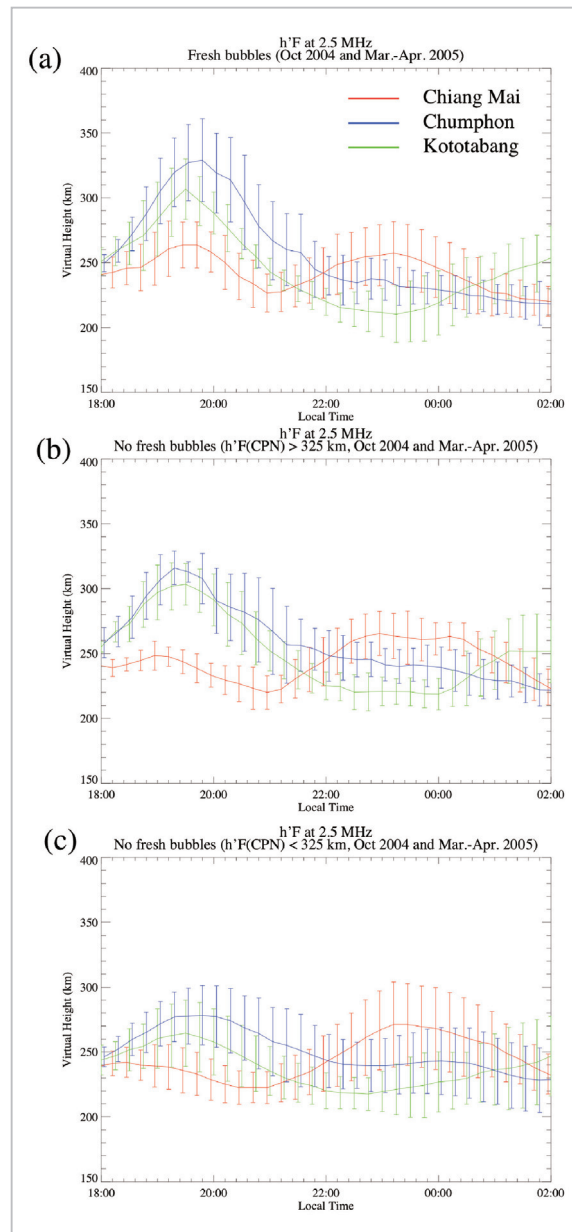


Fig.4 Temporal variations in average h’F at Chumphon (blue), Kototabang (green), and Chiang Mai (red) (a)A “fresh” plasma bubble is observed. (b)A “fresh” plasma bubble was not observed when maximum h’F at Chumphon was 325 km or more. (c)Maximum h’F was less than 325 km at Chumphon [12].

um on days when Chumphon had a significant rise in h’F but witnessed no “fresh” plasma bubbles forming. The value of h’F registered at Chiang Mai in the vicinity of PRE is found systematically lower than that of h’F at Kototabang (line shifted positive), probably

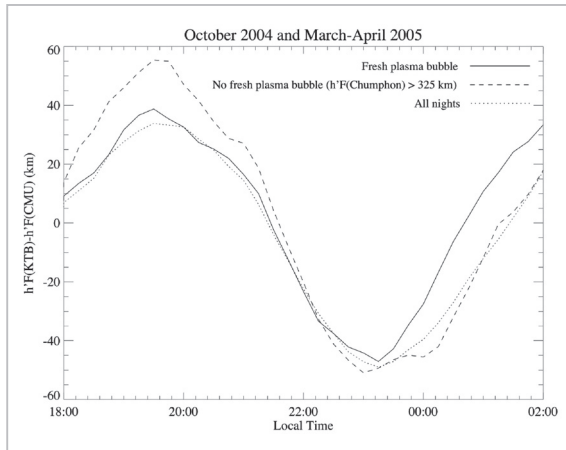


Fig.5 Temporal variations in $h'F$ differences between Kototabang and Chiang Mai. The continuous solid line denotes the observation of a “fresh” plasma bubble, the dashed line the observation of no “fresh” plasma bubbles despite maximum $h'F$ of 325 km or more at Chumphon, and the dotted line the averages calculated in all cases [12].

due to Chiang Mai’s location not being at the precise magnetic conjugate point with Kototabang, but in a slightly higher-latitude region. Kototabang and Chiang Mai are normally located inside the equator anomaly zone, and Chiang Mai—closer to the peak of the equator anomaly zone—generally has a higher electron density but a lower electron isodensity surface beneath the peak. Since the value of $h'F$ used in the present study was read at a constant frequency (2.5 MHz), 2.5 MHz radio waves are reflected at a lower height at Chiang Mai with its higher electron density. Systematic differences in the value of $h'F$ between Kototabang and Chiang Mai can be explained in the following terms:

5 Discussions

Analyses in the present study have revealed that the north-south asymmetrical structure of electron density in the bottomside ionosphere appeared more evident when plasma bubbles did not form despite intense PRE. This is a consequence of suppressing the formation of plasma bubbles in the presence of

an intense degree of north-south asymmetry in electron density of the bottomside ionosphere, suggesting that electron density distributions in the F-region of the bottomside ionosphere that contribute significantly to Pedersen conductivity integrated along magnetic field lines are a key factor governing the formation of plasma bubbles. Increases in Pedersen conductivity integrated along magnetic lines of force act to suppress the non-linear growth of a plasma bubble, as well as PRE itself [1]. Findings of the present survey reveal that the formation of a plasma bubble is suppressed despite strong PRE if the north-south asymmetry is present in electron density of the bottomside ionosphere, thereby suggesting that the formation of a plasma bubble may have been suppressed through suppression of its nonlinear growth rather than PRE.

The height of the F-region of the bottomside ionosphere at the magnetic equator at nighttime is primarily determined by the ionospheric electric field. The drag effect of thermospheric neutral winds along the magnetic meridional plane as mediated by the collision of ions and neutral particles in addition to the electric field plays an important role away from the magnetic equator. Because the magnetic field lines are essentially equipotential in the ionospheric F-region, ionospheric height variations caused by the ionospheric electric field are symmetrical with respect to the magnetic equator. Therefore, the north-south differences in ionospheric height variations may be associated with thermospheric neutral winds blowing along the magnetic meridional plane. Accordingly, the thermospheric neutral wind velocity along the magnetic meridional plane can be derived from temporal changes in $h'F$ at a location remote from the magnetic equator and in the same magnetic meridional plane as the magnetic equator [15]. Because two observation stations are apart from the magnetic equator—one northward and one southward—the thermospheric neutral wind velocity along the magnetic meridional plane can be derived at each of these points to estimate whether the winds tra-

verse the magnetic equator, converge or diverge. The average neutral wind velocities derived in this method were 5 m s^{-1} transequatorially northward when a “fresh” plasma bubble was observed [Fig. 4 (a)], 15 m s^{-1} transequatorially northward when a “fresh” plasma bubble was not observed despite intense PRE [Fig. 4 (b)], and 5 m s^{-1} transequatorially northward with weak PRE, virtually the same value as observed when a “fresh” plasma bubble was observed [Fig. 4 (c)].

Findings of the present study revealed that transequatorial thermospheric neutral winds are a key factor in suppressing the formation of plasma bubbles. This conclusion, however, has not been drawn by analyzing any previous TEC observations [5]–[7]. This difference may be explained in the following terms. According to Maruyama [3][16] and Devasia et al [17], the bottomside ionospheric height or electron density in the bottomside ionosphere that contributes significantly to Pedersen conductivity integrated along magnetic field lines is prerequisite for the formation of a plasma bubble. TEC, on the other hand, is influenced by all ionospheric plasmas present along the path of radio propagation from satellite radio sources to the receivers, with the greatest contribution coming from ionospheric plasma near the peak of the ionospheric F-region, not the bottomside ionosphere. Moreover, electron density distributions above the peak of the ionospheric F-region are significantly influenced by a history of growth in the equatorial anomaly zone since the daytime, as well as the then prevailing thermospheric neutral winds. This fact may well account for the diminished relation between the north-south symmetrical and asymmetrical structures of TEC, and the formation of a plasma bubble.

6 Conclusions

The present study has revealed that transequatorial thermospheric neutral winds are one of the key factors in suppressing the formation of plasma bubbles. Plasma bubbles involve various spatial-scale ionospheric irregularities that could lead to satellite communication failure due to scintillations and degraded differential satellite positioning accuracy resulting from sharp spatial changes in TEC. From a space weather perspective, an ability to forecast the formation of plasma bubbles is urgently needed, but large day-to-day variations in h'F plotted in Fig. 3 and 4 evidently suggest that, besides transequatorial thermospheric neutral winds, various other factors may also be involved in the formation of a plasma bubble. Yet, since the study has suggested that transequatorial thermospheric neutral winds represent a key factor in dominating day-to-day variations of plasma bubble occurrence, a more detailed observation of thermospheric neutral winds may be the next step towards achieving the ability to forecast the formation of plasma bubbles.

Acknowledgements

Ionosonde observations underway at Chiang Mai, Chumphon, and Kototabang have been pursued pursuant to research agreements between the National Institute of Information and Communications Technology (Japan) and Chiang Mai University (Thailand), King Mongkut's Institute of Technology Ladkrabang (Thailand), and Indonesia's National Agency for Aeronautics and Aerospace, respectively. Observations at Kototabang were also conducted with aid from Kyoto University's Research Institute for Sustainable Humanosphere.

References

- 1 Abdu, M. A., "Outstanding problems in the equatorial ionosphere-thermosphere electrodynamics relevant to spread F," *J. Atmos. Solar-Terr. Phys.*, Vol. 63, pp. 869–884, 2001.
- 2 Maruyama, T. and N. Matuura, "Longitudinal variability of annual changes in activity of equatorial spread F and plasma bubbles," *J. Geophys. Res.*, Vol. 89, pp. 10903–10912, 1984.
- 3 Maruyama, T., "Modeling study of equatorial ionospheric height and spread F occurrence," *J. Geophys. Res.*, Vol. 101, pp. 5157–5163, 1996.
- 4 Mendillo, M., J. Baumgardner, X. Q. Pi, P. J. Sultan, and R. T. Tsunoda, "Onset conditions for equatorial Spread F," *J. Geophys. Res.*, Vol. 97, pp. 13865–13876, 1992.
- 5 Mendillo, M., J. Meriwether, and M. Biondi, "Testing the thermospheric neutral wind suppression mechanism for day-to-day variability of equatorial spread F," *J. Geophys. Res.*, Vol. 106, pp. 3655–3663, 2001.
- 6 Valladares, C. E., S. Basu, K. Groves, M. P. Hagan, D. Hysell, A. J. Mazzella Jr., and R. E. Sheehan, "Measurement of the latitudinal distributions of total electron content during equatorial spread F events," *J. Geophys. Res.*, Vol. 106, pp. 29133–29152, 2001.
- 7 Valladares, C. E., J. Villalobos, R. Sheehan, and M. P. Hagan, "Latitudinal extension of low-latitude scintillations measured with a network of GPS receivers," *Ann. Geophys.*, Vol. 22, pp. 3155–3175, 2004.
- 8 Lee, C.-C., J.-Y. Liu, B. W. Reinisch, W.-S. Chen, and F.-D. Chu, "The effects of the pre-reversal drift, the EIA asymmetry, and magnetic activity on the equatorial spread F during solar minimum," *Ann. Geophys.*, Vol. 23, pp. 745–751, 2005.
- 9 Abdu, M. A., K. N. Iyer, R. T. de Medeiros, I. S. Batista, and J. H. A. Sobral, "Thermospheric meridional wind control of equatorial spread F and evening prereversal electric field," *Geophys. Res. Lett.*, Vol. 33, pp. L07106, doi: 10.1029/2005GL024835, 2006.
- 10 Maruyama, T., M. Kawamura, S. Saito, K. Nozaki, H. Kato, N. Hemmakorn, T. Boonchuk, T. Komolmis, and C. Ha Duyen, "Low latitude ionosphere-thermosphere dynamics studies with ionosonde chain in Southeast Asia," *Ann. Geophys.*, Vol. 25, pp. 1569–1577, 2007.
- 11 Maruyama, T., S. Saito, M. Kawamura, K. Nozaki, J. Uemoto, T. Tsugawa, H. Jin, M. Ishii, and M. Kubota, "Outline of the SEALION project and initial results," Special issue of this NICT Journal, 3-2-1, 2009.
- 12 Saito, S. and T. Maruyama, "Ionospheric height variations observed by ionosondes along magnetic meridian and plasma bubble onsets," *Ann. Geophys.*, Vol. 24, pp. 2991–2996, 2006.
- 13 Bittencourt, J. A. and M. A. Abdu, "A theoretical comparison between apparent and real vertical ionization drift velocities in the equatorial F region," *J. Geophys. Res.*, Vol. 86, pp. 2451–2455, 1981.
- 14 Yokoyama, T., S. Fukao, and M. Yamamoto, "Relationship of the onset of equatorial F region irregularities with the sunset terminator observed with the Equatorial Atmosphere Radar," *Geophys. Res. Lett.*, Vol. 31, pp. L24804, doi: 10.1029/2004GL021529, 2004.
- 15 Krishna Murthy, B. V., S. S. Hari, and V. V. Somayajulu, "Nighttime equatorial thermospheric meridional winds from ionospheric h'F data," *J. Geophys. Res.*, Vol. 95, pp. 4307–4310, 1990.
- 16 Maruyama, T., "A diagnostic model for equatorial spread F, 1, Model description and application to electric field and neutral wind effects," *J. Geophys. Res.*, Vol. 93, pp. 14611–14622, 1988.
- 17 Devasia, C. V., N. Jyoti, K. S. V. Subbarao, K. S. Viswanathan, D. Tiwari, and R. Sridharan, "On the plausible linkage of thermospheric meridional winds with the equatorial spread F," *J. Atmos. Solar-Terr. Phys.*, Vol. 64, pp. 1–12, 2002.



SAITO Susumu, Ph.D.

*Senior Researcher, Communication,
Navigation, and Surveillance
Department, Electronic Navigation
Research Institute*

Aeronomy, Satellite Navigation

MARUYAMA Takashi, Ph.D. (Eng.)

*Executive Researcher
Upper Atmospheric Physics*